Detection of Spatter Signature for Streaming Data in the Laser Metal Deposition Process

Muhammad Mu'az Imran[1,2], Gisun Jung[2], Young Kim[2], Azam Che Idris[1], Liyanage Chandratilak De Silva[1], Pg Emeroylariffion Abas[1] and Yun Bae Kim[2]

[1]*Faculty of Integrated Technologies, Universiti Brunei Darussalam, Gadong, Brunei Darussalam*
[2]*Department of Industrial Engineering, Sungkyunkwan University, Suwon, South Korea*

Abstract: In recent years, Laser Metal Deposition (LMD) has experienced significant advancements. For process monitoring purposes, in-situ sensors are often used, which tend to produce noisy data, and due to the short processing window, these data need to be automatically analyzed in real-time to ensure their reliability for further processing. A simple Moving Average (MA) is commonly used to reduce signal peaks, which could otherwise skew the statistical properties of the data. Stabilization of the LMD process can be ascribed to the occurrence of spatters, which exhibit concept drift characteristics and are closely related to signal peaks. In this respect, this study aims to differentiate between two types of anomalies in data streams: point anomalies and concept drift, to eliminate the peaks that could cloak the performance in the actual signals during the process. To solve this issue, a two-step approach is being proposed. A differencing method is first applied to identify any potential point outliers, which are then verified to check if these identified observations are indeed peaks resulting from the spatters generation with a density-distance approach. The method's reliability and robustness were tested with overhang structures (3-axis printing) and impeller blade structures (5-axis printing). Results show that the existing method, the Drift Streaming Peaks-Over-Threshold method, is inferior compared to the proposed method in terms of F1-score, despite a decrease in performance as the inclination angle increases. These experiments ascertain the pertinence of the proposed method in processing incoming sensor data of LMD.

Keywords: Metal Additive Manufacturing, Reasoning-based, Spatter, Statistical Approach, Streaming

1. INTRODUCTION

Laser metal deposition (LMD), also known as Directed Energy Deposition (DED), is one of the common metal Additive Manufacturing (AM) methods available in the market. LMD projects a concentrated energy beam programmed to follow a predetermined toolpath along the given workspace, leaving a trail of solidified weld beads of a particular geometric shape. The intense heat coming from the energy beam, including laser or electron, onto the metal feedstock material in the form of powder or wire, coupled with the substrate, creates a locally liquified melt-pool morphology instantaneously surrounding the vicinity with a rapid solidification process. Unlike traditional manufacturing methods, LMD is capable of freeform fabrication of complex geometries without requiring any support. However, the process often needs consistent and focused energy density in geometrical control because continual irregular powder mass delivery and laser defocusing can cause inconsistency in the build height development [1]. Additionally, the process also involves a multitude of process parameters that directly influence the geometrical and microstructural properties of the finished product. Indeed, it is expected to have occasional defects in the finished products, including a bumpy texture, insufficient deposition, or excessive deposition [2]. One of the methods to improve the quality of an LMD process is via reliable and robust in-situ measurement process and control. The most common in-situ process monitoring is the direct measurement of geometrical characteristics, such as clad height, by obtaining a visual image data using a Charge-Coupled Device (CCD) camera or Complementary Metal-Oxide Semiconductor (CMOS) camera [3]. However, monitoring sensors of the deposition process commonly give noisy time-series data, and since the deposition process occurs rapidly, interpretation of these data and subsequent control of the deposition process can be challenging.

An increasing amount of literature emphasizes the significance of identifying defects or outliers in the field of metal AM. Ren et al. [4] adopted an LSTM-Autoencoder and a K-means clustering to provide early defect detection based on quality classification under different conditions of laser power, printing speed, and powder feed rate. Zhang et al. [5] also used LSTM, but to predict melt pool time-series

temperature during LMD, as the melt pool temperature affects the microstructure of the finished part. On the other hand, Reisch et al. [6] proposed an approach for anomaly detection in multivariate data streams based on the error distance. These errors are then fed to a Mahalanobis distance-based method to generate anomaly scores.

The success yardstick of the monitoring and control model lies in its generalization in capturing intrinsic characteristics of the data. Bartsch et al. [7] asserted that the generalization of a model requires a satisfactory volume of high-quality data, which are representative of the problem, and consisting of only a few outliers and small noise. This manifest in the ability of the model to comprehensively describe the data, in terms of their descriptive patterns and their well-defined characteristics. Outlier detection aims to identify specific data points that significantly deviate from the rest of the dataset, arising from distinct underlying mechanisms. Various types of outliers possess unique statistical characteristics that deviate from normal behaviour, and they might have emerged abruptly or evolved gradually over time. Introducing data containing outliers to a model can have detrimental effects on the model's performance and estimated parameters. Thence, identifying and addressing outliers form a crucial aspect of time series analysis prior to modelling.

Although there are quite a number of methods for detecting peaks in the streaming data application, the reliability of those existing methods is not applicable to the LMD process that presents the non-stationary in the time series data, i.e., noises with process shifts as a new normal. In this case, when a sudden drift develops during the LMD process, it signifies the process is unstable due to a multitude of complex interactions, sensitive to the environment and improper process parameter combinations, thus leading to poor quality. This meaningful information must be retained for downstream analysis, such as characterizing the types of defects based on the features of the signals when process shifts appear. However, to date, existing methods may be overly resistant to these changes, slowly updating their parameters as concept drift appears. Therefore, the central contributions of this study are as the following:

- First, this paper describes the design and implementation of the proposed statistical framework that enables the detection and differentiation between sudden anomalies and drifts in one-dimensional data streams. It is designed explicitly for the LMD process, particularly in industrial practices in both 3-axis and 5-axis printing modes, with the spatter signature—an inextricably linked phenomenon.

- Second, in testing the approach, twenty-seven different unique combinations of parameters of the proposed method were tested to obtain robust and optimal parameters in different scenarios, including both 3-axis and 5-axis printing modes to address spatter

signature effectively—the noise that often interferes with the data—ensuring more accurate and reliable analyses, and

- Third, in numerous industrial instances, detecting abnormalities can be a challenging task. Nevertheless, a recent study highly advocates the use of the Moving Average (MA) coupled with the three-sigma limits (lower and upper limits) approach to classify point anomalies as the actual facts precisely. This method is crucial in resolving the issue and should be put into operation promptly.

The structure of the paper is drafted as follows. Following the introduction to the work in Section 1, Section 2 provides an overview of related works in the area of spatters, concept drift and its detection. The proposed framework is given in Section 3. This includes the proposed outlier detection method as well as the ground truth labelling. Section 4 outlines the experimental setups, as well as results and discussions. The final section concludes the paper.

2. RELATED WORK

A. Spatters and their effects

One of the process-induced defects results from the complex interaction with different mediums, including the selected energy beam, metal feedstock material, and the prior layers, is spatters [8]. Research into spatter behaviour reveals its connection to process conditions and stability, indicating that tracking spatter could provide valuable insights into the quality and consistency of the metal AM process [9], [10], [11], despite being a common phenomenon in LMD. In simple terms, spatter is the expulsion of powder particles that are either melted or unmelted from the melt pool. The purpose of this is to reduce the surface energy. Khairallah et al. [12] provide a comprehensive explanation on the characteristics of the spatter formation in metal AM, which is further investigated by another study that elucidated different sets of process parameters that influence its frequency [13]. Spatter forms when the temperature gradients between the centre and the vicinity of the melt pool are too high due to the higher energy density, i.e., overheating. This higher energy density causes localized boiling on a specific portion of the melt pool, forming a droplet that eventually bursts with an upwards momentum and spread across the surrounding vicinity including the build-part and laser head [14]. Spatter formation strips material from the clad's designed geometry, introducing under-deposition and surface defects such as balling, which in turn exacerbates surface roughness [14]. These imperfections typically necessitate further post-processing, which can prolong the production schedule and inflate costs. When the laser passes by the large spatters settling on the surface of the build-part, it causes insufficient energy density to sufficiently melt the incoming powder and large spatters on the surface simultaneously, contributing to disjointed and sparser solidification [14], [15], [16], potentially giving rise to porosity formation. In addition, it was found that

spatter often precedes with the creation of keyholes [17], a consequence of inappropriately high energy density applied to the substrate or previous layers, which causes overly deep depressions and subsequent voids from gas entrapment. The in-situ monitoring system detected a considerable amount of heavy spattering at the contours [18]. On the built part side, a significant spatter was found, causing substantial disruption to the shape of the melt pool due to defects, such as balling caused by spatters and the separation of the melt. Consequently, the creation of spatters is detrimental to the stability of the process and can result in a myriad of issues, including substandard quality in each layer, porosities, and internal cracks [19].

Rezaeifar and Elbestawi [20] noted that off-axis imaging systems, while measuring the in-situ process of the melt pool size, can suffer from overlapping and spreading spatters, resulting in inaccurate measurements. Thus, it is imperative to mitigate these disturbances to ensure accurate image processing of the melt pool [21]. A few studies have incorporated spatter tracking for denoising as part of an additional step in image processing to reduce these spatter-induced deviations in deposited layer extraction [22], [23]. Further, Feng et al. [24] noted that temperature spikes caused by spatters could lead to potential confusion between defects and noise, emphasizing the need for analysis of temperature signals and interpretation of their results.

According to Hauser et al. [25], there is a strong correlation between spatters and various process parameters. To thoroughly examine this relationship, the study used multi-modal data to acquire image and sound intensity through vision-based and acoustic sensors. The research found that choosing incorrect process parameters can destabilize the process. These errors can ultimately result in significant deviations in the shape of the built layer, which may further cause surface geometry fluctuations and variations in nozzle-to-work distance. These factors can ultimately impact the laser-powder dynamics, leading to more instances of spattering—causing an unstable process, such as spikes in the signals. Additionally, prolonged spatters can lead to concept drift during an unstable process. Despite this, all unstable processes exhibit comparable behaviour in the AE, making distinguishing between them challenging in LMD.

Yang et al. [19] preprocessed the image data to section the melt pool, spatters, and its vicinity represented by pixels in an image. Based on those pixels, they plotted the time series data to monitor the deposition process using the control chart, i.e., Shewhart. The violations of the process stability are indicative of anomalies that might have been incurred during the process. The authors used a moving average to reduce large values that may distort the estimation and smooth out the data points.

In their study, Repossini et al. [26] created a method for analyzing the spattering behaviour during the laser-metal AM process. This method involved measuring the spatters'

characteristics, including area, quantity, and disperseness, to distinguish between under-, normal, and over-melting conditions. The authors suggested that spattering behaviour could be used alongside other known quantities of the melt pool, such as its geometric morphology and temperature, to improve the monitoring process. Similar studies in the field of laser welding [27], [28], [29] have verified that spattering behaviour is one of the critical constituents to characterize the deposition process quality. While there are differences between laser metal AM and laser welding, these studies offer useful insights into characterizing and quantifying spattering behaviour using in-situ signal analysis.

It has been suggested by Chen et al. [30] that complex features can aggravate the frequency of spatters by causing overheating, ultimately leading to more intense spattering. Others have indicated that high laser energy input may also lead to more spattering [25], [30] and larger spatters [19], [30]. Also, Chen et al. [30] utilized Optical Tomography (OT) as an online thermal monitoring tool to label ground truth. Through the analysis of OT images, they were able to infer the effect of layer profiles based on the spatters' frequency produced during the process. The OT images were partitioned into three distinct areas: the section exposed to laser radiation, the region affected by spattering, and the zone unaffected by either laser radiation or spattering. Further analysis compared the frequency and distribution of these regions.

In a nutshell, melt pool instabilities may cause excessive spatters [9], [13], which in turn may cause concept drift in signals [31], [32]. Significantly, it should be highlighted that existing research into the impact of spatter-induced noise and related parameters has predominantly utilized image and sound data. In contrast, the proposed method exclusively employs one-dimensional signal data reflecting the geometric characteristics of the melt pool height. This approach marks a considerable decrease in the computational resources required for analysis.

B. Concept Drift

Data streams are real-time and continuous flows of data, with non-stationary distribution, i.e., distributions may change over time. Unbounded instances of data cannot just be stored all at once in the memory for real-time processing due to computational resource constraints, and this makes it challenging to detect changes in data distribution. However, the summary of these instances can be stored [33]. Another challenge is the speed at which these instances arrive from a stream, which can quickly devour available resources including computational memory. Thus, it is recommended that stream mining algorithms prioritize speed and efficiency by using only a small batch of samples [34].

Concept drift may be defined as a statistical change in observations/distributions. Specifically, given a set of data $S_t = (X_1, \ldots, X_n)$ at a time step t, whereby each sample $X_i = (x_{i,1}, \ldots, x_{i,n})$ is a feature vector. If two consecutive sets of observations S_t and S_{t+1} present a considerable

deviation in the distributions, then it can be said that concept drift appears. The coexistence of concept drifts in the streaming data degrades the classifier's performance over time, making it obsolete for the new incoming instances. Due to this reason alone, tracking this concept's change is essential—underpinning the model's reliability and credibility.

Drift can manifest itself in various ways: suddenly, gradually, incrementally, or repeatedly. Sudden drift is marked by an abrupt alteration in distribution with no overlap between the preceding and present concepts. The new concept may also emerge gradually, with the transition between concepts occurring over time before stabilizing and is referred to as gradual drift. Recurring drift refers to the phenomenon of a concept repeating itself over time with either cyclical or non-cyclical behaviour. In contrast, incremental drift occurs when changes in distribution exhibit a stepwise manner but smoothly and continuously over time. Sudden drift, as the name suggests, is more apparent and noticeable compared to the other types of drift.

C. Outliers and Concept Drift Detection

A change of distribution over time may increase errors in a detection mechanism. As such, the mechanism must be able to trace errors in real time. This research focuses on the removal of extreme values (noise) whilst considering the drift component of the data. In the literature, multiple outlier detection methods exist in streaming data applications, including sequential analysis-based, similarity and dissimilarity-based, window-based, statistically based and data distribution-based [33].

The most commonly used similarity and dissimilarity-based method is the Drift Detection Method (DDM) [35]. DDM embodies two warning levels of detection based on the set confidence interval, i.e., 95% and 99%, respectively. DDM performs well in detecting sudden and gradual drifts but performs atrociously for an incremental drift. Thus, Baena-García et al. [35] proposed an Early-DDM to overcome this challenge. Sequential analysis-based methods, such as the Page-Hinkley Test (PHT) [36], rely on hypothesis testing where incoming signals are assumed to follow a Gaussian distribution. Any sudden changes in variance, either increase or decrease, would be characterized as abnormal. On the other hand, a window-based approach commonly incorporates two windows that accumulate incoming data to form a small batch of data. Differences in the distributions between these two small batches of data may signal a drift. Rather than utilizing a fixed window size, an adaptive window size can be employed to tailor the window size according to the type of drift. A series of multiple statistical-based testing, such as measurements of central tendency, hypothesis testing, kurtosis, and skewness, can also be incorporated into the window-based approach. Vallim and De Mello [37] incorporated a Fourier transform method to produce power spectrum graphs of two sliding windows, before comparing them to detect statistical differences.

Another popular method is the Drift Streaming Peak-Over-Threshold (DSPOT) [38] method, which is based on the data distribution during the initialization phase and iteratively updates the parameters when peaks are detected. The proposed method was rigorously compared to the DSPOT algorithm, which is widely used as a benchmark owing to its popularity. It is worth noting that the DSPOT algorithm is a modified version of the Peaks-Over-Threshold (POT) method that is specifically designed for detecting anomalous points in real-time. Two variants of the POT method were developed by Siffer et al. [38]: Streaming POT and DSPOT. The former is suited for any stationary distribution, while the latter is more robust to handle process shifts in the streaming data. At the outset, the algorithm requires a calibration step to initialize the threshold (quantile) value z_q with a fixed risk q such that $P(X > z_q) < q$. The excess over the threshold (quantile) Th results in a set of peaks $Y_t \leftarrow (X_i - Th \mid X_i > Th)$, with a Generalized Pareto Distribution (GPD) fitted on them to infer z_q. Ultimately, the algorithm can adapt itself to the evolution of data for streaming that can detect anomalies ($X_i > z_q$) and refine z_q. The threshold (quantile) value z_q can be determined as

$$z_q \cong Th + \frac{\widehat{\sigma}}{\widehat{\gamma}}\left(\left(\frac{qn}{N_t}\right)^{-\widehat{\gamma}} - 1\right) \qquad (1)$$

where Th is a high threshold (quantile), n is the total samples, and peaks occurrences over Th is denoted by N_t. Both parameters $\widehat{\sigma}$ and $\widehat{\gamma}$ are estimated through observations using Grimshaw's trick to attain a single-variable function for solving the two variable optimization problems.

It is important to note that whilst DSPOT is robust in other applications, it may not be as effective for the LMD process due to its limitations. Firstly, a large batch of samples is required for the initialization phase before making an inference, including lower and upper bounds to distinguish normal and extreme values. Extreme values that exist in the initialization batch of samples will not be detected because the calibration phase requires a normal state of the process before inferencing the threshold limits. Secondly, if the initialization phase contains many extreme values, it can result in incorrect inference for the threshold limits, i.e., high threshold limits. For instance, if the deposition process begins with excessive spattering behavior, i.e., commonly starts from the edges of the build (contour), the subsequent extreme values during the streaming phase may be missed entirely. Lastly, the method may struggle to adapt to cyclicality in time series, slowly adjusting the threshold value. Therefore, a robust method that is tailored to the LMD process is developed, which will be explained in detail in the next section.

3. METHODOLOGY

When detecting outliers in time-series data, it can be difficult to determine what qualifies as abnormal within the dataset, with outliers having the possibility to disrupt

the outlier detection method. This is even so in LMD, where time-series sequences of an LMD have unique characteristics that make defining anomalies even more challenging [25]. Studies found in the literature have already acknowledged that peaks present in the signal may affect the stability of the process due to spattering events. These events can indicate process stability, but they may also contain information on drift, which is useful for analyzing layer attributes. Care needs to be taken when removing data which are presumed to be outliers, to ensure that only true point anomalies are eliminated while keeping the meaningful spatters. Differentiating concept drift and noise, including extreme values and point anomalies, is a difficult task. For anomaly detection in AM, the control chart method has been employed by researchers to identify anomalies [39], [40], [41], [42], [43], [44], [45]. In the realm of streaming applications, data are in a constant state of flux, posing an even greater challenge to the outlier detection algorithms. Algorithmic models may misidentify noise as concept drift or be excessively resistant to changes. As such, an effective model must maintain a balance of robustness and sensitivity.

A. The Proposed Statistical Framework

In this research, an innovative framework for detecting outliers is introduced that is based on a window-based approach with other statistical techniques, which will be further outlined in this section. As new data streams arrive at the start of every layer, they are collected in a buffer until the buffer's length matches the predefined window size n. Outliers within this smaller batch dataset need to be removed before the start of the streaming phase using Median Absolute Deviation (MAD). During the streaming phase, a differencing method is employed to detect potential outliers within the data stream and subsequently, a density-based outlier detection approach is utilized to confirm whether the detected potential outlier is indeed genuine. If a true outlier is identified, a re-computation phase is triggered, to remove the confirmed outlier in the calculation of the differencing method. This is because an outlier can distort and hide the true outlier as a normal value. Figure 1 depicts a simplified flowchart of the proposed framework.

Batch Processing phase: The batch processing phase occurs at the start of every layer. During the phase, data $x(i)$ are collected in an initial batch X_{init} until it reaches a predefined window size n with $X_{init} = x(1), x(2), \ldots x(n)$. Outliers need to be identified in the initial batch X_{init} to correctly represent the data, and for this, the MAD [46] is used. MAD is a more robust measure of scatteredness in comparison to normal three sigma, which are more sensitive to outliers. Given $M(.)$ as a function that gives median from its input and constant b related to the underlying distribution, $1/Q(0.75)$, MAD can be calculated as

$$MAD = M\left(|x(i) - M(x(i) \in X_{init})|\right) \times b \times \beta, \; x(i) \in X_{init} \quad (2)$$

β is a variable defined by the user, with a high β value

indicating a stricter criterion, and vice versa. Outliers $Y_{init}^{outlier}$ in X_{init} can then be obtained,

$$
\begin{aligned}
Y_{init}^{outlier} \leftarrow &\big\{(x(i) < M(x(i) \in X_{init}) - MAD) \\
&\lor (x(i) > M(x(i) \in X_{init}) + MAD)\big\}, \\
&x(i) \in X_{init}
\end{aligned}
\quad (3)
$$

where $\lor$ is the logical OR operation.

Streaming Phase: A window-based approach is proposed for the efficient handling of the streaming data. Two overlapping sliding windows, $w_0(t)$ and $w_1(t)$, as shown in Figure 2, that differ by one time step are proposed; combinations of which are divided into the detector, counter, and confirmation/verification zones. $w(t)$ indicates the combination of both windows $w_0(t)$ and $w_1(t)$ whilst $w_c(t)$ indicates the count zone of data $x(t)$.

In the detection zone, new data $x(t)$ may be earmarked as a potential outlier according to the difference in data distributions between the two windows. Subsequently, earmarked potential outlier $x_f(t) \equiv x(t)$ is stored in a dictionary F of potential outliers, i.e., $x_f(t) \in F$. In the count zone, the number of succeeding neighbours of the potential outlier $x_f(t) \in F$. In the outliers dictionary F is tallied. Succeeding neighbour is defined as successive data of the potential outlier $x_f(t)$ within the count zone $w_c(t)$, i.e., $x(i) \in w_c(t)$ with values within $x_f(t) \pm R$. Once the potential outlier $x_f(t) \in F$ enters the verification zone, a decision is made to determine if the potential outlier $x_f(t)$ is indeed an outlier, with an outlier defined as those having less than τ succeeding neighbours.

Given a sliding window $w_i(t)$ at time t, with n observations, represented as

$$w_i(t) = \Big\{x(t-(n-1)-i), x(t-(n-2)-i), \ldots x(t-i)\Big\}, \; i = 0, 1 \quad (4)$$

The sliding window $w_i(t)$ can be characterized using its modified moving average $mMA_i(t)$, which can be calculated by excluding data already confirmed as outliers in $Y^{outlier}$,

$$
mMA_i(t) = \frac{\sum_{j=0}^{n-1} |x(t - j - i) - b(t)|}{n}, \\
x(t - j - i) \ni Y^{outlier}, \; i = 0, 1
\quad (5)
$$

where $b(t)$ is the mean of the combined windows $w_0(t)$ and $w_1(t)$ at time t,

$$b(t) = \frac{\sum_{j=0}^{n} x(t - j)}{n}, \quad x(t - j - i) \ni Y^{outlier} \quad (6)$$

The difference $D(t)$ in modified moving average values between the two windows, $w_1(t)$ and $w_0(t)$ can then be easily determined,

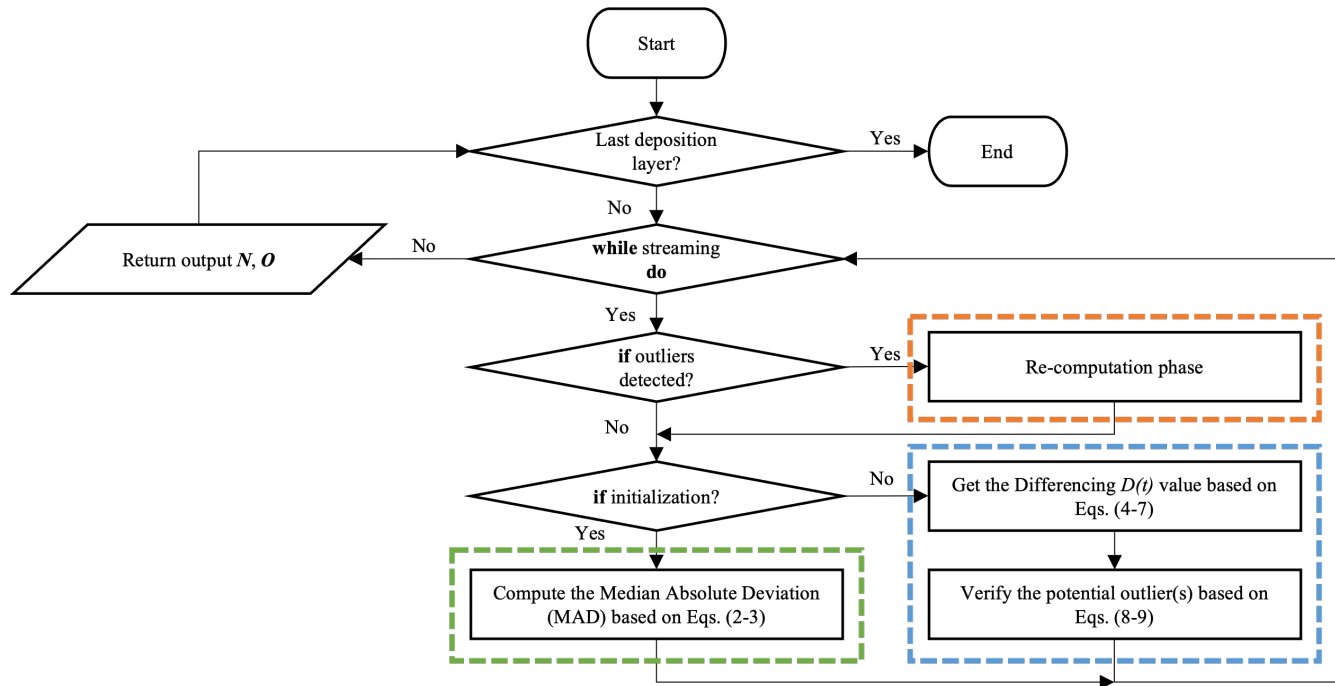$$D(t) = \big|mMA_1(t) - mMA_0(t)\big| \quad (7)$$

Figure 1. The main process flow of the proposed framework, with dashed lines separating different phases: orange in colour represents the re-computation phase, green in colour represents the batch processing, and blue in colour represents the streaming phase
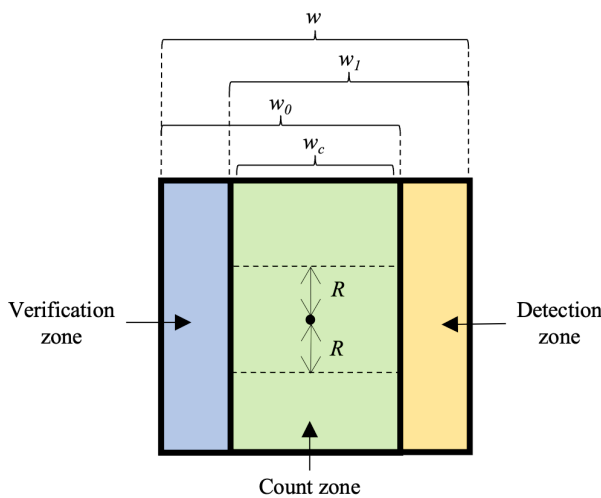

Figure 2. Three different zones of the proposed method consist of the detection zone, count zone w_c with a distance threshold R, and verification zone. These three zones are bounded by the two overlapping sliding windows w_0 and w_1, where w_1 is ahead of the other by 1-time step

$D(t)$ exceeding a pre-determined threshold ρ, i.e., $D(t) > \rho$, indicates that the point $x(t)$ needs to be earmarked as a potential outlier $x_f(t) \equiv x(t)$ and stored in a dictionary F of potential outliers.

A modified density-based approach is then used to

confirm that the potential outlier $x_f(t)$ is indeed an outlier. In the count zone $w_c(t)$, the potential outlier $x_f(t) \in F$ is assigned horizontal rectilinear boundaries set-apart by a length $R \in \mathbb{R}^+$, and these boundaries are used to determine the number of succeeding neighbours $\tau_f(t)$, with values within $\pm R$ range of $x_f(t)$. The calculation of the number of succeeding neighbours $\tau_f(t)$ of potential outlier $x_f(t) \in F$ is done whilst streaming, with $\tau_f(t)$ on the arrival of data $x(i) \in w_c(t)$ determined as,

$$\tau_f(t) \leftarrow \tau_f(t) + f(x(i), x_f(t), R), \qquad x(i) \in w_c(t) \qquad (8)$$

where $f(.)$ is a threshold function defined by

$$f(a, b, c) = \begin{cases} 1 & \text{if } |a - b| \leq C \\ 0 & \text{otherwise} \end{cases} \qquad (9)$$

In the verification zone, if the number of succeeding neighbours $\tau_f(t)$ of potential outlier $x_f(t) \in F$ is smaller than threshold value τ, i.e., $\tau_f(t) < \tau$, the potential outlier $x_f(t)$ is confirmed as an outlier, i.e., $(x_f(t) \equiv x(t)) \in Y^{outlier}$, and vice-versa.

Re-computation phase: In case an outlier has been identified, the process requires re-computation of the difference of mMA values of the data streams. This is because outliers need to be excluded in the calculation of mMA as per equation (5), and the recent confirmation of an outlier necessitates the recalculation of mMA of affected data. Given $(x_f(t) \equiv x(t)) \in Y^{outlier}$ has been confirmed as an outlier in the streaming phase, the re-computation

phase requires re-computation of $D(t_f + 1)$, where t_f is the time index of the recently verified outlier. Similar to the streaming phase, $D(t_f + i)$ exceeding a pre-determined threshold ρ, i.e., $D(t_f + i) > \rho$, necessitates the point $x(t_f + i)$ to be earmarked as a potential outlier, with the number of succeeding neighbours $\tau_f(t_f + i)$ to be recalculated, before the streaming phase can recommence. Figure 3 illustrates the activation of the re-computation phase.
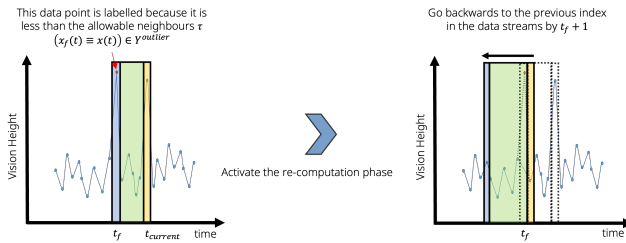

Figure 3. An illustration to show the sliding window w returns to retrograde by $t_f + 1$ to allow for the re-computation phase

An easy-to-understand depiction of this method is presented in Figure 4, showing snapshots at 4 distinct time intervals, with $\tau = 3$ and $n = 5$ set as an example.

B. Ground Truth Labelling

The process of AM involves intricate physical phenomena that include heating, melting, and solidification. These events can affect the dynamics of the process, making it challenging to create a precise labelling procedure. Despite advances in metal AM, there is a shortage of methods for ground truth labelling [47], and there is currently no standard for evaluating the quality of the LMD process for labelling purposes [48].

Measuring the quality of a process can be a tedious and expensive task, whether it is done manually by experts [48], [49], [50] or through post-processing techniques like Computed Tomography (CT) scans [51], [52], or visual inspections [53], especially when done between build layers [52]. Wu et al. [48] devised a meticulous quality evaluation technique based on the three-sigma approach that classifies quality into four tiers, separated by the frequency of spatters. Subsequently, they have also established a correlation between quality levels and the porosity of the finished parts.

This study employs the three-sigma approach, which serves as ground truth and has been used by the study as mentioned above to pinpoint peaks in order to assess the efficacy of the proposed method. In the realm of outlier detection, Recall, Precision, and F1-Score serve as prevalent performance metrics for classification models. Recall gauges the classifier's ability to correctly identify the proportion of true outliers in relation to the total number of outliers. Precision measures the proportion of all outlier predictions that are correct. F1-score combines both precision and recall ratios. The equations for Recall, Precision,

and F1-score are (10), (11), and (12), respectively.

$$Recall = \frac{TP}{TP + FN} \tag{10}$$

$$Precision = \frac{TP}{TP + FP} \tag{11}$$

$$F1 - score = 2 \times \frac{Precision \times Recall}{Precision + Recall} \tag{12}$$

4. RESULTS AND DISCUSSIONS

Experiments were conducted on a MacBook M1 Pro 2021 with 16 GB RAM, using Python 3.9. The goal of these experiments was to effectively identify and manage the process signature that is characterized by high-frequency spatters and process shift components. To gauge its performance, real-world datasets of tilted structures with various slopes ranging from 0° to 10° layers were utilized. The performance of this method was compared with the DSPOT algorithm. Furthermore, the algorithm was tested in the 5-axis printing mode of the impeller blade structure.

A. Experimental Setups

Two different experimentations in 3-axis and 5-axis modes were tested using real experimental data generated from the DLMF DMX 01 (Hwacheon Machinery Co., Ltd, South Korea) as depicted in Figure 5. Inconel 718 alloy powder manufactured by Sandvik with a size range of $53 - 150 \, \mu m$ was used for this experiment. A dual vision-based sensing approach based on CMOS camera sensors was integrated with the DLMF DMX 01, designed with the purpose of acquiring in-situ monitoring of the melt pool height. The details of this sensing technology are built based on the US patent of US7423236B2 [54]. In the 3-axis mode, different overhang structures with different inclination angles from 0° to 10° were constructed. The structures were first constructed with an incline angle of 0° up to $10 \, mm$ in height, after which, a slope of different inclination angles was constructed. The total height of each structure is $30 \, mm$. Overall, there are ten independent overhang structures fabricated. Figure 6(a) and Figure 6(b) show the CAD model and the results of the fabricated overhang structures, respectively. In the 5-axis mode, the impeller blade structure with ten blades and 180 layers, was printed that requires no overhang support as illustrated in Figure 6(c). The process parameters include a fixed z-increment of $0.25 \, mm$, a scanning speed of $850 \, mm/min$, a powder feed rate of $4.5 \, g/min$, and a coaxial gas flow rate of $6.8 \, l/min$. Meanwhile, the laser power was adjusted based on the closed-loop control strategy according to the current melt-pool height. The filling deposition pattern is zigzag with a tool spacing of $0.5 \, mm$.

B. Effect of differencing threshold ρ and linear horizontal boundaries R

Nine out of 27 parameter sets were investigated with the purpose of demonstrating the effects of varying threshold ρ and R values, as tabulated in Table I . Decreasing the ρ value
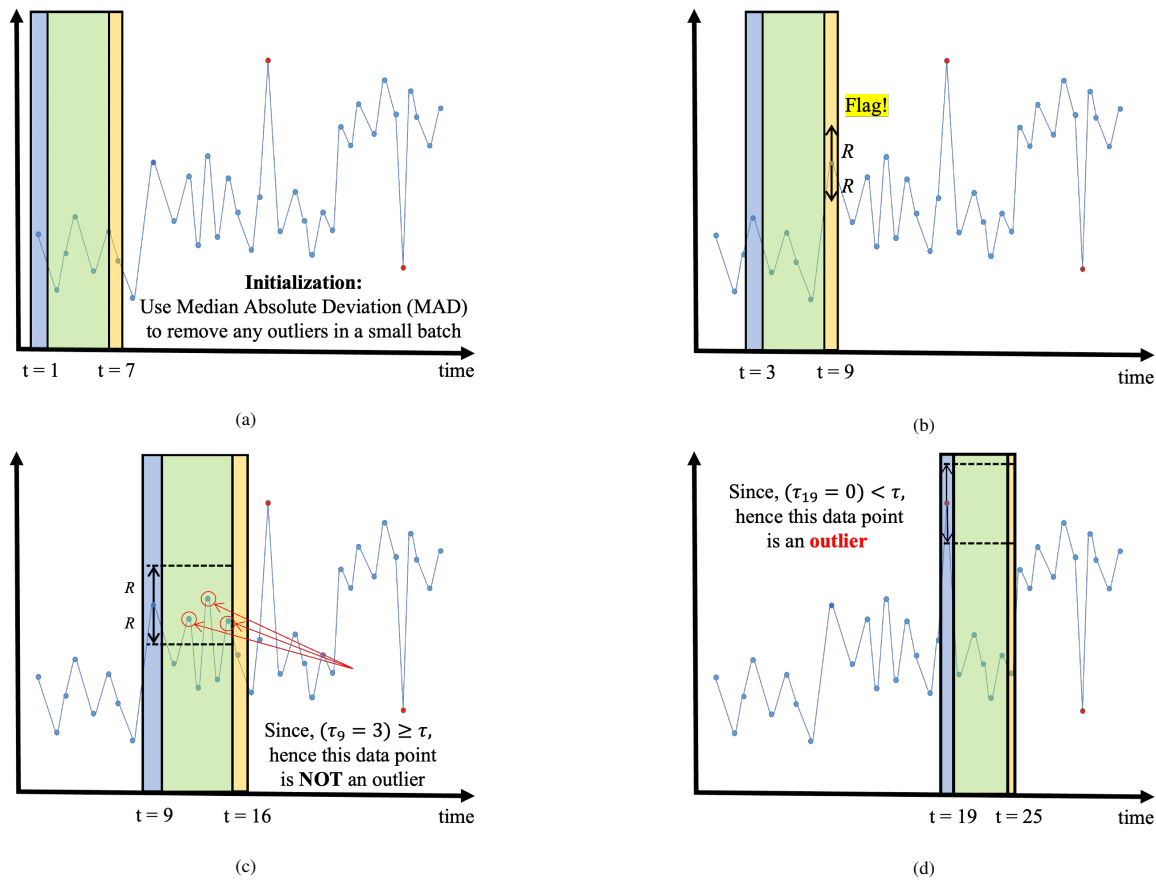
(a)

(b)

(c)

(d)

Figure 4. The proposed method can be visualised by looking at four different time intervals, whilst utilizing sliding windows of length 5 and $\tau = 3$: **(a)** during the batch processing phase, MAD detects outliers in the initial batch X_{init}; **(b)** during the streaming phase, a potential outlier for a window is detected by the differencing method (e.g., x_9 at $t = 9$). This occurs at the detection zone; **(c)** In the subsequent time steps of the count zone, the density-based method tallies up the neighbours of the potential outlier x_9, i.e., $(\tau_9 = 3) \geq \tau$. In the verification zone at $t = 16$, the proposed method cannot confirm that the potential outlier is an outlier, but instead classifies it as concept drift; **(d)** In another scenario, the proposed method confirms that another potential outlier x_{19} is indeed an outlier, with fewer neighbours than the threshold τ
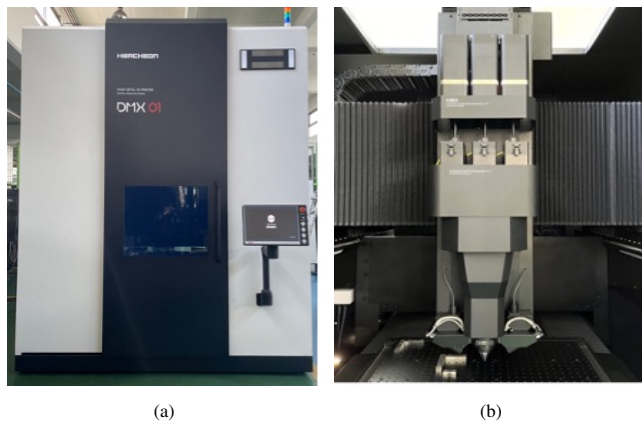

(a)   (b)

Figure 5. DLMF process (Hwacheon Machinery Co., Ltd): **(a)** DMX 01 Metal 3D printer, and **(b)** DMX 01 deposition head

increases recall value. This is because lowering the ρ value increases the detection of potential outliers, thus the more sensitive it gets in detecting the shift in the distributions between the two sliding windows. However, an increase in the number of detected potential outliers also increases computation time in the subsequent verification step. Hence, a compromise between the two metrics (recall and elapsed time) is governed by the proposed framework's forgetting mechanism, which activates the algorithm to backtrack to the detected outlier index $f + 1$ for a recomputation excluding the recently detected outlier. Despite the lower ρ value capable of detecting a high proportion of the true outliers, precision is low as most of the detected outliers are not actual outliers, i.e., high false positives. Since real-time streaming applications require fast computation time, it is necessary to find a balance between the computation time and the overall performance (F1-Score).
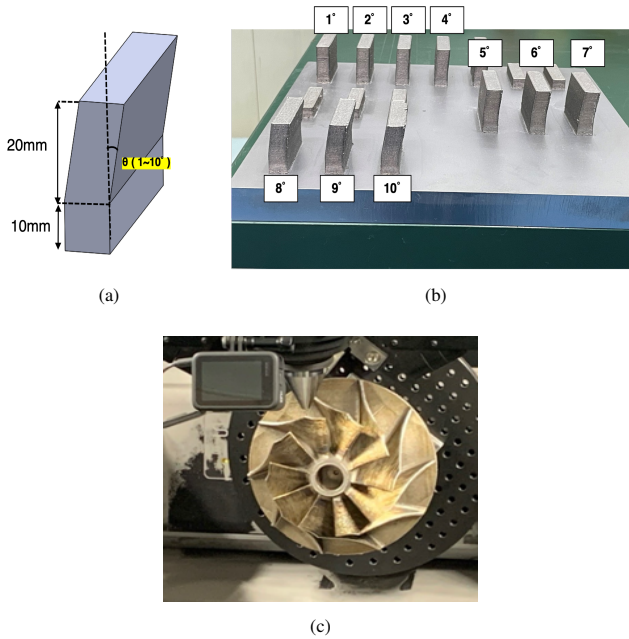
Figure 6. Experimetal datasets: **(a)** The CAD model of the overhang structure; **(b)** The physical artefacts of the overhang structures printed in a 3-axis mode; **(c)** The physical artefact of the impeller blade structure printed in a 5-axis mode

TABLE I. INFLUENCE OF THE DIFFERENCING THRESHOLD ρ and R ($\tau = 3, w = 20$) TO THE PERFORMANCE METRICS AND COMPUTATION TIME. NOTE THAT THIS SENSITIVITY ANALYSIS WAS TESTED ON THE 10° OVERHANG STRUCTURE DATASET (WORST CASE)

Variables	Recall	Precision	F1-Score	Average Elapsed Time (s)
ρ=3,R=50	0.878	0.412	0.561	6.559±2.324
ρ=3,R=75	0.837	0.541	0.657	4.284±1.652
ρ=3,R=100	0.798	0.658	0.721	2.973±1.206
ρ=5,R=50	0.872	0.592	0.705	4.042±1.535
ρ=5,R=75	0.831	0.658	0.734	3.114±1.250
ρ=5,R=100	0.792	0.728	0.759	2.392±0.992
ρ=7,R=50	0.829	0.809	0.819	2.291±1.015
ρ=7,R=75	0.795	0.839	0.816	1.918±0.880
ρ=7,R=100	0.765	0.860	0.810	1.678±0.774

C. Method comparison with overhang structure (3-axis printing mode)

Our method was tested against DSPOT for detecting outliers in real-world overhang structure data, while accounting for concept drift. During the calibration step of the DSPOT algorithm, a large batch of samples (200 samples) was required to obtain z_q, which the inference relies strongly on the excess over a threshold t (high empirical quantile, i.e., 95%) values that follow a Generalized Pareto distribution (GPD).

A comparison group comprising 27 sets of parameters

(ρ, R, τ) combinations of the proposed method with a fixed size window of $w = 20$ alongside the DSPOT algorithm, was analyzed based on their performance metrics, recall, precision, and f1-score, as depicted in Figure 7, Figure 8, and Figure 9, respectively. As mentioned previously, the stability of the LMD process may degrade as the inclination angle increases. This stability can be represented by the spatters formation that results in high peaks of clad height signals. Therefore, finding robust parameters suitable for this volatile incoming streaming data is essential. Figure 7 shows that the DSPOT method is the most stable in terms of recall in which the classifier detects most of the actual outliers, however, suffers greatly in terms of precision, where the numbers of the detected outliers are not actually true, as shown in Figure 8. Especially, with the least sensitive differencing threshold $\rho = 7$, the proposed method performs exceptionally well against the benchmark method, i.e., DSPOT, in detecting the point anomalies.
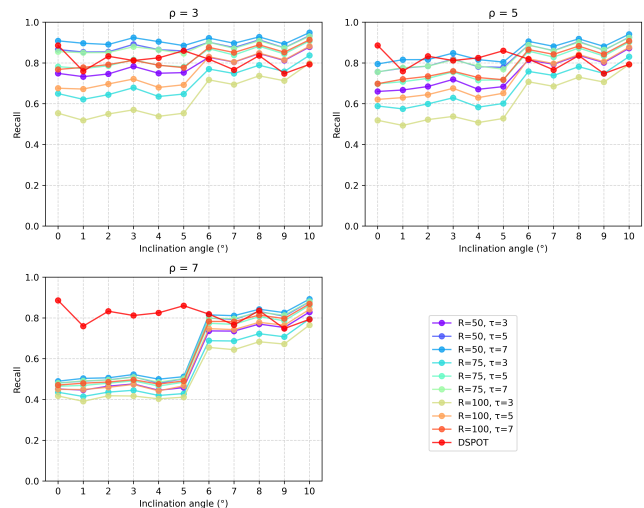

Figure 7. The performance metrics (Recall) between the proposed method with different parameter combinations and DSPOT as a comparison method, with a fixed window size of 20 and different differencing threshold ρ

From the results in Figure 9, it is apparent that the proposed method with the differencing threshold $\rho = 5$, provides the most stable f1-score (less volatile), over the range of tested inclination angles. What is striking about the results in Figure 8 and Figure 9 is that this particular set of parameters is better than the benchmark in terms of precision and f1-score over the range of inclination angles. Although the DSPOT method gives slightly higher recall results than the proposed method with the particular set of parameters in the case of 0° to 5° inclination angles, the precision of the proposed method outperforms the DSPOT method. Retrospective to the aim of outlier detection defined in this study is to locate and eliminate peaks in the streaming data that are regarded as noise from spatters generation. As a result, precision takes precedence over recall. It is vital to accurately remove this noise while
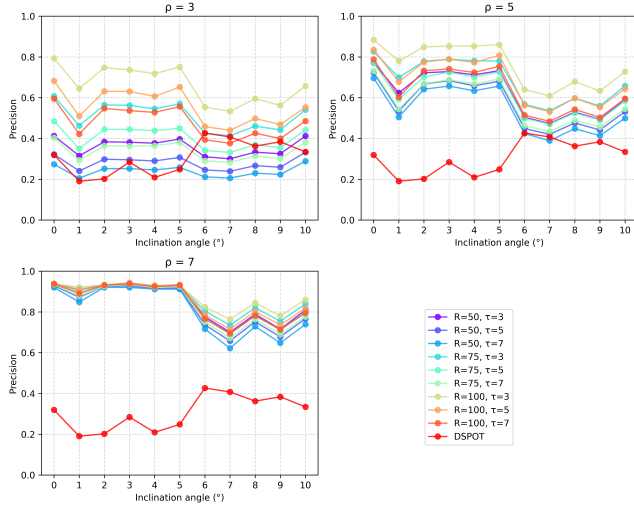
Figure 8. The performance metrics (Precision) between the proposed method with different parameter combinations and DSPOT as a comparison method, with a fixed window size of 20 and different differencing threshold ρ
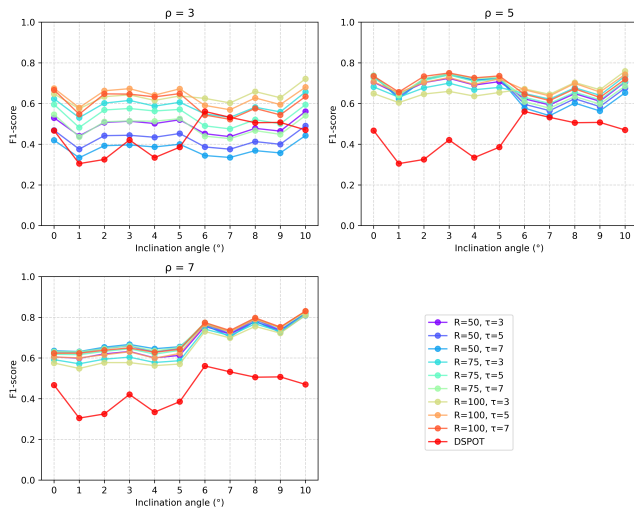

Figure 9. The performance metrics (F1-score) between the proposed method with different parameter combinations and DSPOT as a comparison method, with a fixed window size of 20 and different differencing threshold ρ

preserving the significant spatters that result in process shifts in the streaming data as an indicator for subsequent analysis, such as anomaly detection. Moreover, in the 0° structure, the parameter of $\rho = 5, R = 75$ and, $\tau = 7$ yields the highest f1-score of 0.738, with a recall of 0.756 and a precision of 0.731. In the 10° structure, the parameter of $\rho = 7, R = 100$ and, $\tau = 7$ yields the highest f1-score of 0.830, with a recall of 0.869 and a precision of 0.795.

Furthermore, the results obtained from averaging the relevant metrics values of all inclination angles were summarized in Figure 10, Figure 11, and Figure 12, respectively.

These figures rank the proposed method with different parameter combinations and the DSPOT method in descending order (top to bottom) in terms of performance. From Figure 10, it can be seen that the DSPOT method sits nearly at the bottom, exhibiting its higher recall in detecting most of the actual outliers. At the same time, the proposed method still performs better than the DSPOT with the set of parameters of $\rho = 3, R = 50$ and, $\tau = 7$, attaining the highest recall value. In addition, Figure 11 and Figure 12 are quite revealing in several ways. First, it demonstrates ostentatiously that, in terms of precision and f1-score, the DSPOT method underperforms the proposed framework. The highest average precision is from the proposed method with a set of parameters of $\rho = 7, R = 100$ and, $\tau = 3$. Finally, a set of parameters of $\rho = 7, R = 75$ and, $\tau = 7$ appears to be the most robust in terms of the overall balance between recall and precision of different inclination angles, including the worst-case scenario (10°), and henceforth, this set of parameters was utilized.
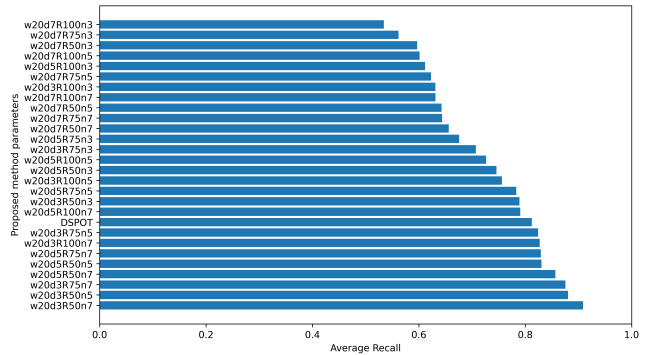

Figure 10. Average recall values of all parameters, sorted in descending order (The highest value is at the bottom, and the lowest value is at the top)
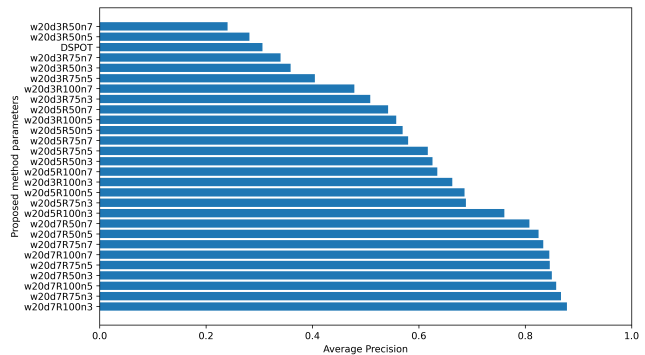

Figure 11. Average precision values of all parameters, sorted in descending order (The highest value is at the bottom, and the lowest value is at the top)

Figure 13 presents the two methods' layerwise analysis of the time-series clad height signals alongside the outcomes of these figures are depicted in the form of a confusion matrix, with Table II summarizing the performance scores of our and benchmark methods. It can be seen the time-
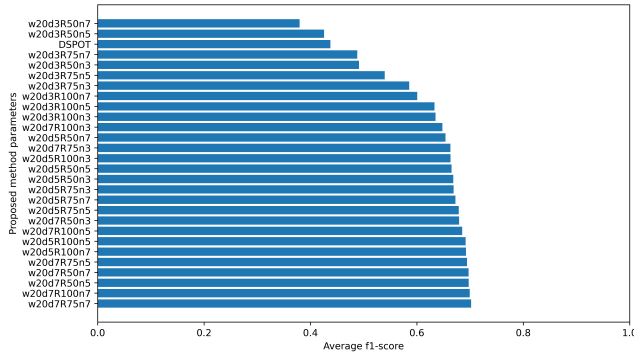
Figure 12. Average f1-score values of all parameters, sorted in descending order (The highest value is at the bottom, and the lowest value is at the top)

TABLE II. THE PERFORMANCE METRICS LAYERWISE COMPARISON RESULTS BETWEEN THE PROPOSED METHOD ($\rho = 7, R = 75, \tau = 7, w = 20$) AND THE DSPOT METHOD

Angle	Method	Recall	Precision	F1-score	Elapsed Time (s)
0°	**Proposed**	0.574	0.938	0.712	0.798 ± 0.434
	DSPOT	0.886	0.347	0.499	4.300 ± 4.065
10°	**Proposed**	0.880	0.776	0.825	2.744 ± 1.191
	DSPOT	0.793	0.334	0.470	2.806 ± 4.437

series data of a 10° inclination angle has many extreme values (point anomalies) and is more prone to concept drift compared to 0°. This difference in the occurrence of high peaks shows that fabricating complex structures without support intensifies the spatter formation.

The emergence of concept drift is more pronounced at the layer with a 10° inclination angle, i.e., near the start and end of the signal. The DSPOT method performs poorly at the layer with a 10° inclination angle because, during the calibration step, there are too many extreme values; thus, it sets the z_q to be too high. Due to this miscalibration, the upper threshold was set way too high and despite gradually diminishing, it persistently settled above the remaining peaks, leading to missing out on many true outliers, as shown in Figure 13(e). On the other hand, if extreme values are less; z_q is set too low, resulting in lower upper and lower thresholds (orange dashed lines) as shown in Figure 13(d). Due to this, the DSPOT method misclassified many false positive outliers in the initial phase of the layer build process. Figure 13(f) shows that the DSPOT algorithm has trouble adapting to the concept drift in the initial and end phases due to changes in mean value. Thus, it detects the normal signals as false positive outliers. On the other hand, the proposed method handles this problem well. Even with concept drift, the proposed

method flags the point shift as a potential outlier, with the verification zone confirming otherwise.

In addition, in cases where the benchmark technique detects multiple peaks in the streaming data, it must perform a recalculation of sigma and gamma using Grimshaw's trick to achieve a numerical root finding. As a result, the optimization problem of DSPOT takes longer to complete than our proposed forgetting mechanism. Table II showcases the elapsed time required for our method with a 0° inclination angle using the proposed method takes 0.798 ± 0.434 seconds only, while the DSPOT requires 4.300 ± 4.065 seconds. Despite the computation time for the DSPOT algorithm being comparable with the proposed method for the 10° inclination angle, the f1-score of the DSPOT is too low at 0.470 as it failed to detect most of the true outliers, as compared to 0.825 by the proposed method. Irrespective, the elapsed time for our method is still low with low variance.

Furthermore, Table II displays that the f1-scores of our method are better than the benchmark method at both angles. At 0° inclination angle, our method gave recall, precision, and F1-score values of 0.574, 0.938, and 0.712, respectively, compared to the benchmark method, which gave the values of 0.886, 0.347, and 0.499, respectively. Although the recall value of the benchmark method is higher than the proposed method at 0° inclination angle, the precision value of the proposed method scores a near-perfect 1.0, with fewer false positive outliers, whereas the DSPOT method scores 0.347 in terms of precision. Together these results provide important insights into considering the right balance between recall and precision; detecting the noise (extreme values) is more critical during the data acquisition, as it could conceal the actual performance of the deposition process. Meanwhile, the meaningful spatters' presence in the signals is meant to be kept for further analysis, such as characterizing defects based on the different types of concept drifts in the LMD process. The signals of the 10° inclination angle show the presence of gradual, incremental, and recurrent concept drifts. Due to this, the performance of the proposed method is decreased, although it remains higher than the benchmark method.

D. Method comparison with impeller blade structure (5-axis printing mode)

The proposed method with parameters $\rho = 7, R = 75$ and, $\tau = 7$ obtained from analysis of the 3-axis mode and the DSPOT method with parameters $q = 0.001, N_{init} = 200, w = 20$, were tested on another real experimental data of the 5-axis printing mode of the impeller blade dataset for comparisons. The results of the experiment comprising all stated metrics, including the average layerwise elapsed time, are summarized in Table III.

The average scores for the entire blades were also computed and compared between the two methods. Ten different blades were segregated for the analysis, and the performance of our method was averaged with recall, precision, and f1-score calculated at 0.964, 0.512, and 0.668,
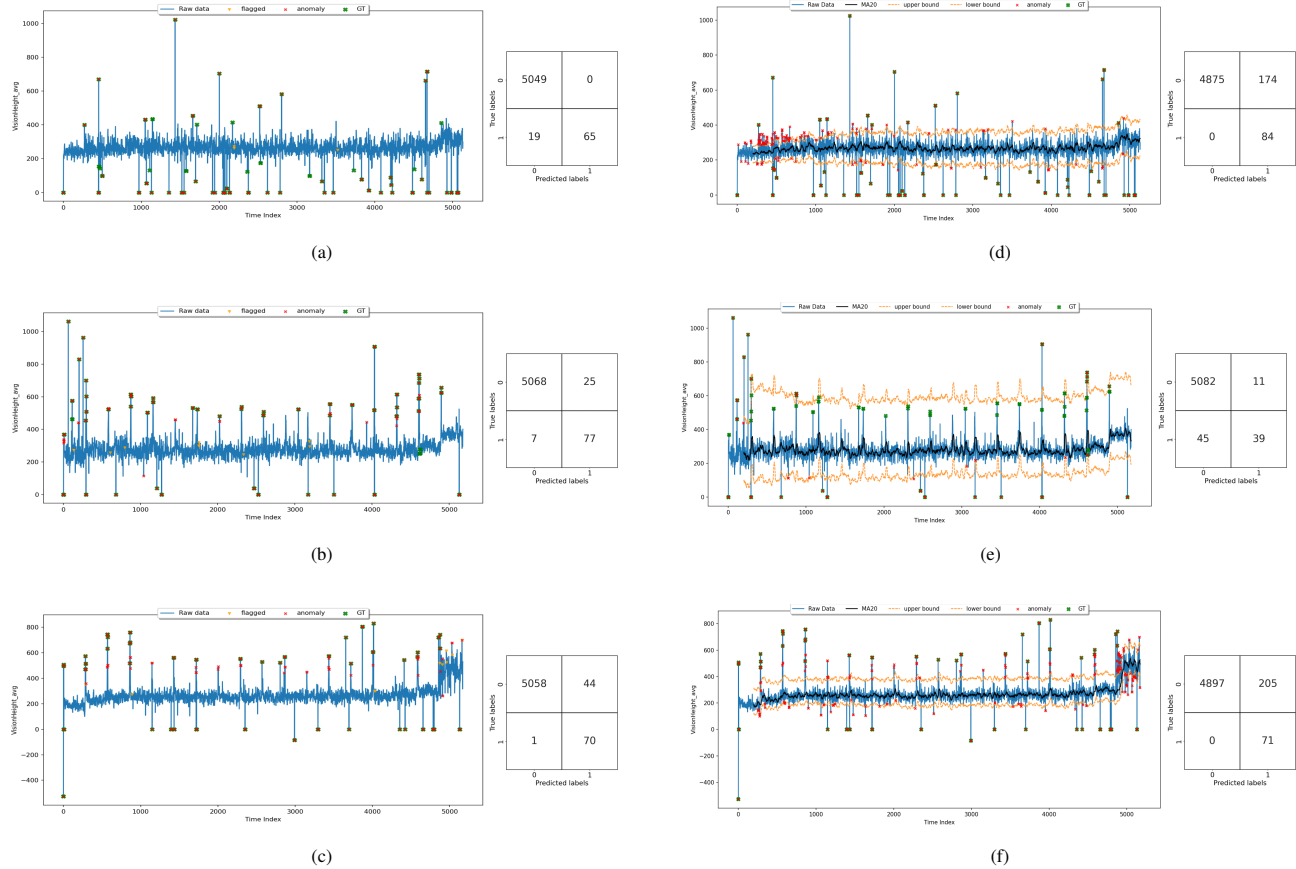
(a)

(d)

(b)

(e)

(c)

(f)

Figure 13. The visualization of the time-series of clad height and its corresponding confusion matrix at three different layers of the 3-axis overhang dataset by two different methods: **(a-c)** Differencing, ($\rho = 7, R = 75, \tau = 7, w = 20$), show a rendering of raw signal (blue), point ground truth (green), point flagged (orange), and point anomaly (red); **(e-f)** DSPOT, ($q = 0.001, N_{init} = 200, w = 20$), show a rendering of raw signal (blue), moving average (black), lower and upper bounds (orange), point ground truth (green), and point anomaly (red); at layer 2 (0°), layer 63 (10°), and layer 69 (10°), respectively

respectively. The average layerwise computation times on the 5-axis are relatively fast, as there are not as many extreme values due to the absence of overhang deposition requirement on the 5-axis printing mode, which is around 0.0976 ± 0.336 seconds. Another reason may be that the printing deposition is lessened as the layer grows. Thus, it eases the printing process for complex structures. However, it is best to note that the 5-axis printing and 3-axis printing are not entirely the same, as the layer thickness varies in the 5-axis mode, which may result in different time-series characteristics of the clad height signals, as depicted in Figure 14. In sum, an interesting finding that stands out from the results reported earlier from the 3-axis overhang dataset was our method transcends the benchmark method in all scores approximately by 6%, 134.7%, 116%, and 153% difference, in terms of recall, precision, f1-score, and the average layerwise computation time, respectively.

These unanticipated results can be further explicated based on the layerwise visualization between our and benchmark methods for detecting the point anomalies, as illustrated in Figure 14. For blade #0 (layer 1), the DSPOT

method is found to have difficulty in adapting to the cyclicality type of time series—slowly adjusting the lower and upper bounds—resulting in detecting more false positive outliers as compared to our method, from 80 to 26, respectively. This description can be analyzed in Figure 14(a) and Figure 14(d). At the same time, detecting these false positive outliers also results in higher computation time in the DSPOT due to Grimshaw's trick calibration. A closer inspection of Figure 14(e) shows that the DSPOT method is not stable when the variance of the signals is high leading to higher false positives, thus lower precision. Finally, the most interesting aspect of this 5-axis result is shown in Figure 14(f) which shows that the DSPOT method fails to adapt to slow decreasing trend type of drift. One of the apparent limitations of the proposed method is that it may struggle when the signal has a high variance, as shown in Figure 14(b). Thus, the proposed method misclassified these small peaks as spatter noise. Despite this shortcoming, the proposed method still outperforms the benchmark method, DSPOT.

In a broader context of AM quality control and process

TABLE III. THE PERFORMANCE METRICS OF THE OVERALL LAYERS OF EACH IMPELLER BLADE RESULTS BETWEEN THE PROPOSED METHOD ($\rho = 7, R = 75, \tau = 7, w = 20$) AND THE DSPOT METHOD

Blade #ID	Method	Recall	Precision	F1-score	Average Elapsed Time (s)
0	**Proposed**	**0.96394**	**0.49922**	**0.65778**	**0.09376 ± 0.29378**
	DSPOT	0.90144	0.10563	0.18911	0.78041 ± 1.20691
36	**Proposed**	**0.96695**	**0.50528**	**0.65437**	**0.09627 ± 0.37592**
	DSPOT	0.89902	0.10028	0.18043	0.71426 ± 0.95754
72	**Proposed**	**0.96453**	**0.49515**	**0.65778**	**0.09888 ± 0.35032**
	DSPOT	0.89184	0.11230	0.19948	0.77470 ± 1.13434
108	**Proposed**	**0.95845**	**0.50662**	**0.66286**	**0.09922 ± 0.34288**
	DSPOT	0.88161	0.11243	0.19943	0.75873 ± 1.03328
144	**Proposed**	**0.95970**	**0.50471**	**0.66152**	**0.09002 ± 0.29851**
	DSPOT	0.91438	0.11288	0.19943	0.75466 ± 1.2959
180	**Proposed**	**0.96901**	**0.51784**	**0.67498**	**0.09441 ± 0.28228**
	DSPOT	0.89583	0.10253	0.18400	0.77104 ± 1.39730
216	**Proposed**	**0.97705**	**0.63986**	**0.77330**	**0.10441 ± 0.43713**
	DSPOT	0.94184	0.21801	0.35406	0.71570 ± 1.08659
252	**Proposed**	**0.96376**	**0.47839**	**0.63940**	**0.09754 ± 0.33639**
	DSPOT	0.89772	0.10940	0.19504	0.70409 ± 1.14212
288	**Proposed**	**0.95380**	**0.48340**	**0.64162**	**0.10213 ± 0.31208**
	DSPOT	0.89883	0.12495	0.21940	0.75548 ± 1.17494
324	**Proposed**	**0.96679**	**0.48660**	**0.64737**	**0.09898 ± 0.32944**
	DSPOT	0.91040	0.09491	0.17190	0.74331 ± 1.08522
Average	**Proposed**	**0.96440**	**0.51171**	**0.66769**	**0.09756 ± 0.33587**
	DSPOT	0.90329	0.11933	0.20938	0.74724 ± 1.15141

optimization, it is crucial to differentiate between point anomalies, which are merely spatter as noise, and concept drift, which is prolonged spatter leading to an unstable process, during data acquisition in laser metal-based AM. This distinction is critical for an accurate quality control assessment. For instance, spatters can create transient spikes in data acquisition signals when evaluating layer deposition performance, whether layer-wise or voxel-wise [55]. These spikes can be mistakenly categorized as anomalies but are actually noise resulting from the natural process of laser-based metal AM. Such a false positive evaluation on localized regions can be misinterpreted as anomalies by the AM controller; failure to address these issues would lead to a false decision on the region and ultimately cause the inception of defects, which can propagate as the layers grow in the z-direction. This false decision poses a severe threat to the integrity of the fabricated component. For example, in order to enhance the geometric precision of each layer, deviations from the standard are categorized as under-deposition, normal, or over-deposition and color-coded accordingly. If the melt pool height signals, contaminated by spatter-induced noise, indicate multiple instances of over- and under-deposition in certain areas, feeding this data into the Convolutional Neural Network (CNN) model could result in misclassification of layer performance as abnormal. Therefore, the proposed method is essential for a reliable data acquisition process and, thus, efficient quality control in laser metal-based AM; otherwise, the defective fabricated component has to be scrapped, leading to wastage in materials and an increase in production lead time.

Many methods for removing spatter involve analyzing 2D images of the melt pool geometry through image processing. However, this research emphasizes the use of one-dimensional time series data and an efficient proposed algorithm, which is more efficient in terms of computing power and can be applied in real-time scenarios. The practical implementation of the method necessitates the integration of CMOS camera sensors with a compatible processor and software suite for real-time data analysis [56]. A prime example of an effective setup involves leveraging the Beckhoff TwinCAT3 system alongside Beckhoff TwinCAT Analytics, powered by the C69xx series Industrial PCs, in tandem with a Beckhoff Control Panel. This configuration presents a robust control platform for AM applications, especially when combined with TwinCAT software on a Windows 10 environment, utilizing an Intel® Core™ processor. The Beckhoff TwinCAT3 system is designed to facilitate real-time visualization of the manufacturing process, enhancing human-machine interaction through web-based processing. This enables comprehensive analysis, visualization, diagnosis, and documentation of both external and internal process variables. Meanwhile, Beckhoff TwinCAT Analytics serves as a potent tool for the synchronization of process data in real-time streams, proving essential for straightforward and insightful process analysis. The capability to extend the software framework with C/C++ and MATLAB, through integration with Mathworks toolboxes for machine learning and optimization, significantly amplifies the analytical capabilities of the setup. The suite encompasses a diverse range of algorithms aimed at analyzing both live and
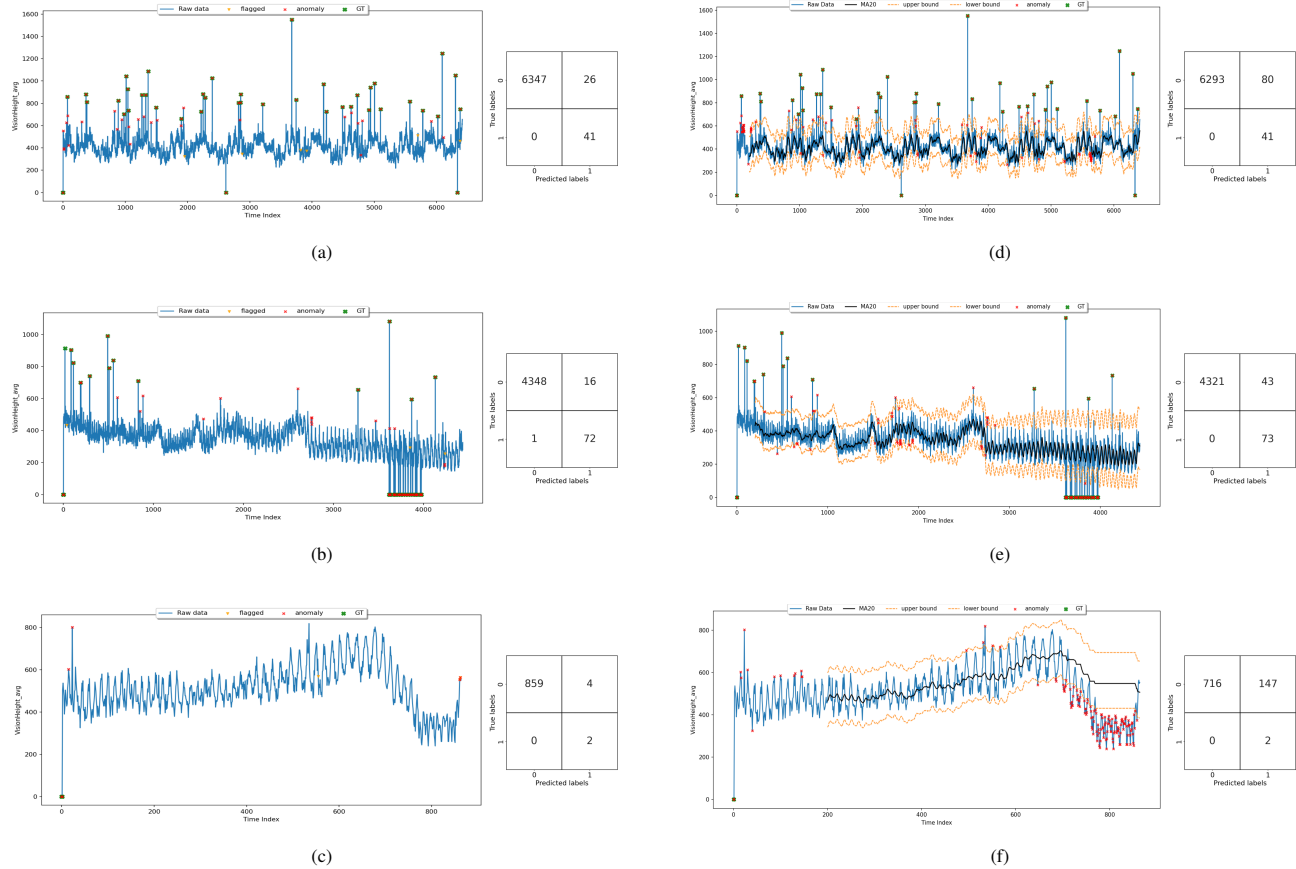
Figure 14. The visualization of the time-series of clad height at three different layers of the 5-axis impeller blade dataset by two different methods: **(a-c)** Differencing, ($\rho = 7, R = 75, \tau = 7, w = 20$), show a rendering of raw signal (blue), point ground truth (green), point flagged (orange), and point anomaly (red); **(d-f)** DSPOT, ($q = 0.001, N_{init} = 200, w = 20$), show a rendering of raw signal (blue), moving average (black), lower and upper bounds (orange), point ground truth (green), and point anomaly (red); of blade #0 (layer 1), blade #180 (layer 2), and blade #324 (layer 94), respectively

historical data across single or multiple distributed systems, specifically designed for in-depth data analysis. This configuration has been successfully applied in the context of fused filament fabrication technologies, incorporating computer vision-based quality control mechanisms to enhance the manufacturing of AM components [57]. Consequently, adopting this proven configuration for the deployment of the proposed method appears both practical and feasible.

5. CONCLUSIONS AND FUTURE WORK

During the LMD process, spatter can pose a significant challenge and negatively impact process stability. High-frequency spatters can cause signal peaks that obscure the true performance of the deposition process. A novel approach that integrates differencing and density-based methods was developed to combat this issue and simultaneously reduce noise from univariate time series data. This involves comparing two modified Moving Averages to identify potential outliers, which are then confirmed using a density-based method that considers neighbouring data points. To test the effectiveness of this approach, the study employed actual datasets of 3-axis overhanging structures with various

inclination angles and 5-axis impeller blade structures. The DSPOT method was used as a benchmark, and the three-sigma approach coupled with the moving average was used to label peaks in the signal as the ground truth. The proposed method was then evaluated against twenty-seven different parameters to determine the optimal option, which proved to perform exceptionally well in various scenarios. The results revealed that our method outperformed the benchmark in all metrics, including recall, precision, f1-score and computational time. However, finding optimal parameters for different scenarios that involve high-frequency spatter at a 10° inclination angle remains a challenge. It was found that the proposed method with a high ρ yields higher precision when tested on the inclination angles below 5° but at the cost of a low recall, i.e., many missed out outliers. Nonetheless, the lower ρ would result in a slight increase in recall but at the cost of higher computation time because it flags up many potential outliers, i.e., increased sensitivity. Another challenge is handling the combination of recurrent and incremental drifts, i.e., a cyclic of a slow and gradual drift, often appearing at the 10° structure and

impeller blade structure, i.e., complex structures. Hence, the decline in the proposed model performance, including the DSPOT method.

It is worth considering that the proposed method has a limitation in that the parameters (ρ, R, τ) require fine-tuning to achieve optimal results. In the current study, only the 3-axis mode was fine-tuned, and the resulting optimal parameters were applied to the 5-axis impeller blade scenario. However, this may not necessarily be the most effective approach, i.e., suboptimal. To ensure the robustness of the proposed method, future work should explore different structures and conduct independent fine-tuning for each scenario. Moving forward, it is imperative that we thoroughly analyze and provide in-depth comparison evaluations that may affect the robustness of our method when utilizing a variety of static and adaptive window sizes with complex build structures. The generalization of static window size is found to be not robust enough for different scenarios, given the different types of concept drift that may exist, such as gradual, incremental, and recurring drifts, or even a high variance in the signal. Additionally, exploring and implementing an improvement for the forgetting mechanism could significantly increase computational speed through parallel computation.

ACKNOWLEDGEMENTS

REFERENCES

[1] F. Kaji, H. Nguyen-Huu, A. Budhwani, J. A. Narayanan, M. Zimny, and E. Toyserkani, "A deep-learning-based in-situ surface anomaly detection methodology for laser directed energy deposition via powder feeding," *Journal of Manufacturing Processes*, vol. 81, pp. 624–637, 2022.

[2] M. Liu, A. Kumar, S. Bukkapatnam, and M. Kuttolamadom, "A review of the anomalies in directed energy deposition (ded) processes & potential solutions - part quality & defects," *Procedia Manufacturing*, vol. 53, pp. 507–518, 2021.

[3] W.-W. Liu, Z.-J. Tang, X.-Y. Liu, H.-J. Wang, and H.-C. Zhang, "A review on in-situ monitoring and adaptive control technology for laser cladding remanufacturing," *Procedia CIRP*, vol. 61, pp. 235–240, 2017.

[4] W. J. Ren, G. R. Wen, Z. F. Zhang, and J. Mazumder, "Quality monitoring in additive manufacturing using emission spectroscopy and unsupervised deep learning," *Materials and Manufacturing Processes*, vol. 37, no. 11, pp. 1339–1346, 2022.

[5] Z. Y. Zhang, Z. C. Liu, and D. Z. Wu, "Prediction of melt pool temperature in directed energy deposition using machine learning," *Additive Manufacturing*, vol. 37, 2021.

[6] R. Reisch, T. Hauser, B. Lutz, M. Pantano, T. Kamps, and A. Knoll, "Distance-based multivariate anomaly detection in wire arc additive manufacturing," in *2020 19th IEEE International Conference on Machine Learning and Applications (ICMLA)*. IEEE, 2020, pp. 659–664.

[7] K. Bartsch, A. Pettke, A. Hübert, J. Lakämper, and F. Lange, "On the digital twin application and the role of artificial intelligence in additive manufacturing: a systematic review," *Journal of Physics: Materials*, vol. 4, no. 3, p. 032005, 2021.

[8] M. Grasso and B. M. Colosimo, "Process defects and in situ monitoring methods in metal powder bed fusion: a review," *Measurement Science and Technology*, vol. 28, no. 4, p. 044005, 2017.

[9] P. R. Gradl, O. R. Mireles, C. S. Protz, and C. P. Garcia, *Metal Additive Manufacturing for Propulsion Applications*, ser. AIAA Progress in Astronautics and Aeronautics Book Series. American Institute of Aeronautics & Ast, 2022.

[10] D. Wang, Y. Yang, Y. Liu, Y. Bai, and C. Tan, *Formation Mechanism of Spatter and Its Influence on Mechanical Properties in Process of Laser Powder Bed Fusion*. Springer, 2023, pp. 135–177.

[11] M. Qu, Q. Guo, L. I. Escano, A. Nabaa, S. M. H. Hojjatzadeh, Z. A. Young, and L. Chen, "Controlling process instability for defect lean metal additive manufacturing," *Nature communications*, vol. 13, no. 1, p. 1079, 2022.

[12] S. A. Khairallah, A. T. Anderson, A. Rubenchik, and W. E. King, "Laser powder-bed fusion additive manufacturing: Physics of complex melt flow and formation mechanisms of pores, spatter, and denudation zones," *Acta Materialia*, vol. 108, pp. 36–45, 2016.

[13] H. S. Prasad, F. Brueckner, and A. F. Kaplan, "Powder incorporation and spatter formation in high deposition rate blown powder directed energy deposition," *Additive Manufacturing*, vol. 35, p. 101413, 2020.

[14] D. Svetlizky, M. Das, B. Zheng, A. L. Vyatskikh, S. Bose, A. Bandyopadhyay, J. M. Schoenung, E. J. Lavernia, and N. Eliaz, "Directed energy deposition (ded) additive manufacturing: Physical characteristics, defects, challenges and applications," *Materials Today*, vol. 49, pp. 271–295, 2021.

[15] S. Wang, J. Ning, L. Zhu, Z. Yang, W. Yan, Y. Dun, P. Xue, P. Xu, S. Bose, and A. Bandyopadhyay, "Role of porosity defects in metal 3d printing: Formation mechanisms, impacts on properties and mitigation strategies," *Materials Today*, 2022.

[16] Z. Li, H. Li, J. Yin, Y. Li, Z. Nie, X. Li, D. You, K. Guan, W. Duan, and L. Cao, "A review of spatter in laser powder bed fusion additive manufacturing: In situ detection, generation, effects, and countermeasures," *Micromachines*, vol. 13, no. 8, p. 1366, 2022.

[17] L. Wang, Y. Zhang, H. Y. Chia, and W. Yan, "Mechanism of keyhole pore formation in metal additive manufacturing," *npj Computational Materials*, vol. 8, no. 1, p. 22, 2022.

[18] T.-T. Ikeshoji, M. Yonehara, C. Kato, Y. Yanaga, K. Takeshita, and H. Kyogoku, "Spattering mechanism of laser powder bed fusion additive manufacturing on heterogeneous surfaces," *Scientific Reports*, vol. 12, no. 1, p. 20384, 2022.

[19] L. Yang, L. Lo, S. Ding, and T. Özel, "Monitoring and detection of meltpool and spatter regions in laser powder bed fusion of super

alloy inconel 625," *Progress in Additive Manufacturing*, vol. 5, pp. 367–378, 2020.

[20] H. Rezaeifar and M. Elbestawi, "Minimizing the surface roughness in l-pbf additive manufacturing process using a combined feedforward plus feedback control system," *The International Journal of Advanced Manufacturing Technology*, vol. 121, no. 11-12, pp. 7811–7831, 2022.

[21] J. Ning, Y. Zhao, L. Zhu, C. Yang, M. Yu, Z. Yang, S. Qin, Z. Jiang, L. Xu, and J. Li, "Height consistency compensation in laser-directed energy deposition of thin-walled parts," *International Journal of Mechanical Sciences*, vol. 266, p. 108963, 2024.

[22] B. Li, Y. Zhang, Y. Lei, H. Wei, C. Chen, F. Liu, P. Zhao, and K. Wang, "A single-sensor multi-scale quality monitoring methodology for laser-directed energy deposition: Example with height instability and porosity monitoring in additive manufacturing of ceramic thin-walled parts," *Additive Manufacturing*, vol. 79, p. 103923, 2024.

[23] M. Slodczyk, A. Ilin, T. Kiedrowski, T. Bareth, and V. Ploshikhin, "Spatter reduction by multi-beam illumination in laser powder-bed fusion," *Materials & Design*, vol. 212, p. 110206, 2021.

[24] W. Feng, Z. Mao, Y. Yang, H. Ma, K. Zhao, C. Qi, C. Hao, Z. Liu, H. Xie, and S. Liu, "Online defect detection method and system based on similarity of the temperature field in the melt pool," *Additive Manufacturing*, vol. 54, p. 102760, 2022.

[25] T. Hauser, R. T. Reisch, T. Kamps, A. F. Kaplan, and J. Volpp, "Acoustic emissions in directed energy deposition processes," *The International Journal of Advanced Manufacturing Technology*, pp. 1–16, 2022.

[26] G. Repossini, V. Laguzza, M. Grasso, and B. M. Colosimo, "On the use of spatter signature for in-situ monitoring of laser powder bed fusion," *Additive Manufacturing*, vol. 16, pp. 35–48, 2017.

[27] D. You, X. Gao, and S. Katayama, "Visual-based spatter detection during high-power disk laser welding," *Optics and Lasers in Engineering*, vol. 54, pp. 1–7, 2014.

[28] X.-d. Gao, W. Qian, and S. Katayama, "Analysis of high-power disk laser welding stability based on classification of plume and spatter characteristics," *Transactions of Nonferrous Metals Society of China*, vol. 23, no. 12, pp. 3748–3757, 2013.

[29] M. Zhang, G. Chen, Y. Zhou, S. Li, and H. Deng, "Observation of spatter formation mechanisms in high-power fiber laser welding of thick plate," *Applied Surface Science*, vol. 280, pp. 868–875, 2013.

[30] Z. Chen, A. Raza, and E. Hryha, "Influence of part geometry on spatter formation in laser powder bed fusion of inconel 718 alloy revealed by optical tomography," *Journal of Manufacturing Processes*, vol. 81, pp. 680–695, 2022.

[31] H. Yan, M. Grasso, K. Paynabar, and B. M. Colosimo, "Real-time detection of clustered events in video-imaging data with applications to additive manufacturing," *IISE Transactions*, vol. 54, no. 5, pp. 464–480, 2022.

[32] P. Zhang, X. Zhou, H. Ma, J. Hu, Y. He, X. Wang, and Y. Duan, "Anomaly detection in laser metal deposition with photodiode-based melt pool monitoring system," *Optics & Laser Technology*, vol. 144, p. 107454, 2021.

[33] S. Agrahari and A. K. Singh, "Concept drift detection in data stream mining: A literature review," *Journal of King Saud University-Computer and Information Sciences*, vol. 34, no. 10, pp. 9523–9540, 2022.

[34] S. Wares, J. Isaacs, and E. Elyan, "Data stream mining: methods and challenges for handling concept drift," *SN Applied Sciences*, vol. 1, pp. 1–19, 2019.

[35] M. Baena-Garcıa, J. del Campo-Ávila, R. Fidalgo, A. Bifet, R. Gavalda, and R. Morales-Bueno, "Early drift detection method," in *Fourth international workshop on knowledge discovery from data streams*, vol. 6. Citeseer, 2006, pp. 77–86.

[36] H. Mouss, D. Mouss, N. Mouss, and L. Sefouhi, "Test of page-hinckley, an approach for fault detection in an agro-alimentary production system," in *2004 5th Asian control conference (IEEE Cat. No. 04EX904)*, vol. 2. IEEE, 2004, pp. 815–818.

[37] R. M. Vallim and R. F. De Mello, "Proposal of a new stability concept to detect changes in unsupervised data streams," *Expert systems with applications*, vol. 41, no. 16, pp. 7350–7360, 2014.

[38] A. Siffer, P.-A. Fouque, A. Termier, and C. Largouet, "Anomaly detection in streams with extreme value theory," in *Proceedings of the 23rd ACM SIGKDD international conference on knowledge discovery and data mining*, 2017, pp. 1067–1075.

[39] Y. Li, J. Polden, Z. Pan, J. Cui, C. Xia, F. He, H. Mu, H. Li, and L. Wang, "A defect detection system for wire arc additive manufacturing using incremental learning," *Journal of Industrial Information Integration*, vol. 27, p. 100291, 2022.

[40] Z. Ye, C. Liu, W. Tian, and C. Kan, "In-situ point cloud fusion for layer-wise monitoring of additive manufacturing," *Journal of Manufacturing Systems*, vol. 61, pp. 210–222, 2021.

[41] S. Fathizadan, F. Ju, and Y. Lu, "Deep representation learning for process variation management in laser powder bed fusion," *Additive Manufacturing*, vol. 42, p. 101961, 2021.

[42] B. Bevans, A. Ramalho, Z. Smoqi, A. Gaikwad, T. G. Santos, P. Rao, and J. Oliveira, "Monitoring and flaw detection during wire-based directed energy deposition using in-situ acoustic sensing and wavelet graph signal analysis," *Materials & Design*, vol. 225, p. 111480, 2023.

[43] S. C. Jensen, J. D. Carroll, P. R. Pathare, D. J. Saiz, J. W. Pegues, B. L. Boyce, B. H. Jared, and M. J. Heiden, "Long-term process stability in additive manufacturing," *Additive Manufacturing*, vol. 61, p. 103284, 2023.

[44] Y. Zhang, S. Shen, H. Li, and Y. Hu, "Review of in situ and real-time monitoring of metal additive manufacturing based on image processing," *The International Journal of Advanced Manufacturing Technology*, vol. 123, no. 1-2, pp. 1–20, 2022.

[45] B. M. Colosimo, "Quality monitoring and control in additive manufacturing," in *Wiley StatsRef: Statistics Reference Online*. Wiley, 2020, pp. 1–7.

[46] C. Leys, C. Ley, O. Klein, P. Bernard, and L. Licata, "Detecting outliers: Do not use standard deviation around the mean, use absolute deviation around the median," *Journal of experimental social psychology*, vol. 49, no. 4, pp. 764–766, 2013.

[47] R. Leach, D. Bourell, S. Carmignato, A. Donmez, N. Senin, and

W. Dewulf, "Geometrical metrology for metal additive manufacturing," *CIRP annals*, vol. 68, no. 2, pp. 677–700, 2019.

[48] Z. Wu, Z. Xu, and W. Fan, "Online detection of powder spatters in the additive manufacturing process," *Measurement*, vol. 194, p. 111040, 2022.

[49] D. Cannizzaro, A. G. Varrella, S. Paradiso, R. Sampieri, E. Macii, E. Patti, and S. Di Cataldo, "Image analytics and machine learning for in-situ defects detection in additive manufacturing," in *2021 Design, Automation & Test in Europe Conference & Exhibition (DATE)*. IEEE, 2021, pp. 603–608.

[50] J. Akhavan, J. Lyu, and S. Manoochehri, "A deep learning solution for real-time quality assessment and control in additive manufacturing using point cloud data," *Journal of Intelligent Manufacturing*, pp. 1–18, 2023.

[51] X. Li, X. Jia, Q. Yang, and J. Lee, "Quality analysis in metal additive manufacturing with deep learning," *Journal of Intelligent Manufacturing*, vol. 31, pp. 2003–2017, 2020.

[52] C. Gobert, E. W. Reutzel, J. Petrich, A. R. Nassar, and S. Phoha, "Application of supervised machine learning for defect detection during metallic powder bed fusion additive manufacturing using high resolution imaging," *Additive Manufacturing*, vol. 21, pp. 517–528, 2018.

[53] G. Masinelli, S. A. Shevchik, V. Pandiyan, T. Quang-Le, and K. Wasmer, "Artificial intelligence for monitoring and control of metal additive manufacturing," in *Industrializing Additive Manufacturing: Proceedings of AMPA2020*. Springer, 2021, pp. 205–220.

[54] J.-H. Suh, "Method and system for real-time monitoring and controlling height of deposit by using image photographing and image processing technology in laser cladding and laser-aided direct metal manufacturing process," 2008.

[55] M. M. Imran, Y. Kim, G. Jung, L. C. De Silva, J.-H. Suh, P. E. Abas, and Y. B. Kim, "In-situ process monitoring and defects detection based on geometrical topography with streaming point cloud processing in directed energy deposition," *IEEE Access*, vol. 11, pp. 131 319–131 337, 2023.

[56] A. Elkaseer, M. Salama, H. Ali, and S. Scholz, "Approaches to a practical implementation of industry 4.0," in *The Eleventh International Conference on Advances in Computer-Human Interactions ACHI 2018*, 2018.

[57] R. Nascimento, I. Martins, T. A. Dutra, and L. Moreira, "Computer vision based quality control for additive manufacturing parts," *The International Journal of Advanced Manufacturing Technology*, vol. 124, no. 10, pp. 3241–3256, 2023.

Muhammad Mu'az Imran is a Ph.D. student in the Faculty of Integrated Technologies and the Department of Industrial Engineering at Universiti Brunei Darussalam (UBD) and Sungkyunkwan University, respectively. He completed his undergraduate study at the Faculty of Integrated Technologies, UBD, with a major in Manufacturing Systems Engineering. His research interests are spatiotemporal analysis, machine learning application, metal additive manufacturing, and population synthesis.

Young Kim is a Ph.D. student in the Department of Industrial Engineering at Sungkyunkwan University. He received B.Eng. degree in System Management Engineering from Sungkyunkwan University. He is currently interested in simulation-based modeling, forecasting method, statistical analysis, and population synthesis.

Gisun Jung is a Postdoctoral researcher in the Department of Industrial Engineering at Sungkyunkwan University. He received a Ph.D. degree in Industrial Engineering from Sungkyunkwan University and a B.Eng. degree in System Management Engineering from Sungkyunkwan University. He is interested in demand forecasting, modeling and simulation Methodology, data analytics based on stochastic processes, and machine learning.

Azam Che Idris is an assistant professor at the Universiti Brunei Darussalam. He graduated from the University of Manchester in 2013 with a doctorate degree in aerospace engineering. Before joining Universiti Brunei Darussalam, he was a senior lecturer of the Mechanical Engineering department at the National Defence University of Malaysia. His research includes computational fluid dynamics machine learning applications.

Liyanage Chandraktilak De Silva received BSc Eng (Hons) degree from the University of Moratuwa Sri Lanka in 1985, an Mphil degree from the Open University of Sri Lanka in 1989, Meng and Ph.D. degrees from the University of Tokyo, Japan in 1992 and 1995 respectively. Currently, he is a Professor and the Dean at the School of Digital Science, Universiti Brunei Darussalam. His current research interests are signal processing (speech and image), the Internet of Things, Sensor Integration, and Power System analysis.

Pg Emeroylariffion Abas received a B.Eng. degree in information systems engineering and a Ph.D. degree in communication systems from Imperial College, London, in 2001 and 2005, respectively. He is currently a Senior Assistant Professor in system engineering with the Faculty of Integrated Technologies, Universiti Brunei Darussalam. His current research interests are data analysis, security of info-communication systems, and the design of photonic crystal fiber in fiber optics communication.

Yun Bae Kim is a Professor at the Department of Industrial Engineering at Sungkyunkwan University. He received an MS degree from the University of Florida and a Ph.D. degree from Rensselaer Polytechnic Institute, New York. His current research interests are metal additive manufacturing focusing on directed energy deposition process, demand forecasting, simulation methodology, epidemiology simulation modeling, high-tech market analysis, and scheduling.